

Article

Analysis of the Influence Mechanism of Nanomaterials on Spontaneous Imbibition of Chang 7 Tight Reservoir Core

Xiaoxiang Wang ¹, Yang Zhang ², Xinmeng Wu ³, Xin Fan ², Desheng Zhou ^{1,*} and Jinze Xu ^{1,4} 

¹ School of Petroleum Engineering, Xi'an Shiyou University, Xi'an 710065, China; 180617@xsyu.edu.cn (X.W.); jinz Xu@ucalgary.ca (J.X.)

² Oil Production Plant 11 of PetroChina Changqing Oilfield Company, Qingyang 745000, China; zhangsyu2021@126.com (Y.Z.); xinfan003@126.com (X.F.)

³ South Sulige Operating Company of CNPC Changqing Oilfield, Xi'an 710018, China; wuxinm_cq@petrochina.com.cn

⁴ Department of Chemical and Petroleum Engineering, University of Calgary, Calgary, AB T2N 1N4, Canada

* Correspondence: dzhou@xsyu.edu.cn

Abstract: This study investigates the impact of nanomaterials on different surfactant solutions. By measuring the parameters (including emulsification property, zeta potential, DLS, CA, IFT, etc.) of imbibition liquid system with nanoparticles and without nanoparticles, combining with imbibition experiments, the law and mechanism of improving the imbibition recovery of nanomaterials were obtained. The findings demonstrate that the nano-silica sol enhances the emulsification and dispersion of crude oil in the surfactant system, resulting in smaller and more uniform particle sizes for emulsified oil droplets. Non-ionic surfactant AEO-7 has the best effect under the synergistic action of nanomaterials. Zeta potential and DLS tests also showed that AEO-7 exhibits smaller particle sizes due to their insignificant electrostatic interaction with nanoparticles. Furthermore, the addition of nanomaterials enhances the hydrophilicity of core and reduces the interfacial tension. Under the synergistic action of nanoparticles, AEO-7 still showed the best enhanced core hydrophilicity (CA 0.61° after imbibition) and the lowest interfacial tension (0.1750 mN·m⁻¹). In the imbibition experiment, the imbibition recovery of the system with nanomaterials is higher than that of the non-nanomaterials. The mixed system of AEO-7 and nano-silica sol ZZ-1 has the highest imbibition recovery (49.27%). Combined with the experiments above, it shows that nanomaterials have a good effect on enhancing the recovery rate of tight core, and the synergistic effect of non-ionic surfactant AEO-7 with nanomaterials is the best. Moreover, nanomaterials reduce adhesion work within the system while improving spontaneous imbibition recovery. These findings provide theoretical guidance for better understanding the mechanism behind nanomaterial-induced imbibition enhancement as well as improving tight oil's imbibition recovery.

Keywords: tight oil; spontaneous imbibition; nanomaterials; surfactants



Citation: Wang, X.; Zhang, Y.; Wu, X.; Fan, X.; Zhou, D.; Xu, J. Analysis of the Influence Mechanism of Nanomaterials on Spontaneous Imbibition of Chang 7 Tight Reservoir Core. *Processes* **2024**, *12*, 890. <https://doi.org/10.3390/pr12050890>

Academic Editor: Urszula Bazylińska

Received: 18 March 2024

Revised: 23 April 2024

Accepted: 23 April 2024

Published: 27 April 2024



Copyright: © 2024 by the authors. Licensee MDPI, Basel, Switzerland. This article is an open access article distributed under the terms and conditions of the Creative Commons Attribution (CC BY) license (<https://creativecommons.org/licenses/by/4.0/>).

1. Introduction

Tight oil reservoirs exhibit unfavorable physical properties, complex pore-throat structure, low permeability, and significant heterogeneity. In the process of exploration and development, there are problems of low effective utilization rate and primary recovery [1], which are proved by Wang Xuewu et al. [2–4], and the oil recovery is determined by porosity, permeability, wettability, and other factors. The Chang 7 reservoir is located in the Ordos Basin, with superior hydrocarbon source rock conditions, tight reservoir, complex pore structure, and high oil saturation. Spontaneous imbibition is a good method to improve the recovery of tight oil reservoirs [5,6] because of a high capillary force which is the main driving force of spontaneous imbibition. The study by Li Chuanliang et al. [7–13] proves that surfactants have a positive effect on improving recovery due to their excellent performance in reducing the contact angle and reducing the interfacial tension between

oil and water. The imbibition experiments and imbibition mechanisms of different types of surfactant systems have been extensively studied [14–16]. The most widely accepted mechanisms are reduced contact angle, reduced interfacial tension, emulsification, etc. Nanofluids, considered a “new star material” in the petroleum field, are increasingly favored by researchers. At present, the nanoparticles commonly used to enhance oil recovery are SiO_2 , Al_2O_3 , MgO , TiO_2 , and so on [17–22]. Some scholars [23] have studied the application of MoS_2 nanosheets in enhanced oil recovery. Gong et al. [24] developed a novel nanocomposite polymer fracturing fluid system, which has good temperature resistance and shear resistance, strong sand carrying capacity, and low residue content after rubber breaking. Many scholars have also conducted research on the mechanism of the enhanced oil recovery of nanomaterials [17–22,25]. Suleimanov et al. [18] conducted nano-dispersion experiments and pointed out that nanomaterials can effectively reduce the interfacial tension (IFT) between oil and water phases, which increases the recovery of crude oil by 35%. Some scholars propose that nanofluids possess a higher potential for enhancing recovery compared to single surfactant solutions because nanofluids have a unique “structure separation pressure” characteristic compared with ordinary inhalants, which makes it easier to displace oil droplets from the rock surface, and has better performance on enhanced oil recovery [26]. The important mechanism of nanomaterials in the process of oil–water displacement—wedge extrusion effect—was first proposed by Chaudhury [27]. Many scholars in the world have revealed the excellent performance of nanomaterials in enhancing oil recovery [20,21]. Although nanomaterials hold vast application prospects in oilfield development, further theoretical support is required to integrate them with field practice. Based on the above investigation, we experimentally studied the performance and imbibition of the surfactant system with nanoparticles and non-nanoparticles, aiming to conduct a more in-depth study on the imbibition of nanoparticles on the surfactant system and provide a theoretical foundation for applying nanomaterials in tight oil reservoir exploitation.

2. Materials and Methods

In this paper, we use cores from the Chang 7 reservoir. The basic physical property parameters, including mineral composition and content, porosity, permeability, wettability, etc., are measured to illustrate the physical property of the core. The stability of the different imbibition liquid systems with nanoparticles and non-nanoparticles was studied by emulsification and dispersion experiments. The zeta potential and DSL tests were also conducted to clarify the stability and particle size of the system. Finally, the imbibition recovery was obtained by an imbibition experiment. Through the analysis of the correlation between the imbibition recovery rate and the parameters of the imbibition liquid system above, the mechanism of the nanomaterials in spontaneous imbibition to enhance the recovery rate is obtained.

2.1. Materials and Instruments

The cores, imbibition fluids, and instruments used for the experiment are shown below.

- (1) Cores: The 6 cores selected for this study are all from the Chang 7 reservoir. Table 1 shows the petrophysical parameters which are obtained from laboratory measurements. Following the oil and gas industry standard of the People’s Republic of China “Oil and Gas Reservoir Evaluation Method” (SY/T 6285-2011), the rock porosity and permeability values are extremely low, indicating that they belong to low-pore, ultra-low permeability core.
- (2) Imbibition liquid system: The imbibition solution system consisted of a combination of surfactant and nan-silica sol. The surfactants used were anionic sodium dodecyl sulfate (SDS), amphoteric lauric amide propyl betaine (LAB), and Fatty alcohol polyoxyethylene ether AEO-7 (AEO-7), all at a concentration of 0.2%. The nanomaterial

used was silica sol with a mass fraction of 30%, particle size ranging from 10 to 20 nm, and a concentration of 0.1%, which is numbered as ZZ-1.

Table 1. Physical property parameters of cores and imbibition fluids.

Core Number	Length/cm	Diameter/cm	Permeability/mD	Porosity/%	Initial Wetting Angle/°	Imbibition Fluid System
1	4.326	2.527	0.7921	12.31	22.63	SDS
2	4.289	2.530	0.8304	12.34	10.94	LAB
3	4.276	2.516	0.9585	12.89	25.81	AEO-7
4	4.278	2.526	0.7694	12.08	11.71	SDS + ZZ-1
5	4.420	2.520	0.8315	12.38	15.30	LAB + ZZ-1
6	4.163	2.552	0.9435	12.21	11.80	AEO-7 + ZZ-1

- (3) Simulated formation water: Referring to the field configuration of the Chang 7 reservoir, the water composition is NaCl-based with a total salinity of 25,000 mg/L. It exhibits a density of 1.0108 g/cm³ and a viscosity of 3.60 mPa·s.
- (4) Simulated formation oil: A mixture comprising kerosene and oil red has been utilized, displaying a density of 0.8714 g/cm³, viscosity of 3.92 mPa·s, and exhibiting a distinct red appearance.
- (5) Instruments: The instruments used in this study is shown in Table 2.

Table 2. Instruments used in study.

Number	Instrument Name	Instrument Model
1	X-ray diffraction apparatus	Ultima IV, Rigaku, Japan
2	Magnetic resonance imaging system	Mecro MR23-060H-I, Suzhou Niumai Electronic Technology Co., LTD, China
3	Scanning electron microscope	JSM-5500LV, JEOL, Japan
4	Microscope	OLYMPUS-CX33, Beijing Leibo Ruijie Technology Co., LTD, China
5	Contact angle measuring instrument	HARKE-SPCA, China
6	Rotary drop interfacial tensiometer	KRUSS site100, Germany
7	Zetasizer nano series	Nano-ZS90, Malvern instruments, UK

2.2. Experimental Methods

(1) Test of rock mineral composition and analysis of pore structure

X-ray diffraction spectrum (XRD): The core is ground into a powder and is dried at a low temperature. About 10 g of the samples is filled into the groove of the sample frame for testing.

Nuclear magnetic resonance (NMR): The T_2 spectrum of the standard core is tested, and the pore size distribution curve of the core is calculated according to the relaxation rate of the pore surface.

Scanning electron microscope (SEM): The core is made into a thin film of about 10 mm × 10 mm, and then polished by argon ion beam after mechanical polishing, and observed by SEM.

(2) Emulsification and dispersion of crude oil in imbibition fluid systems

Equal volumes of the imbibition fluid and crude oil are added to the test tube, and the oil and water are shaken up and down until they are fully mixed. After standing for 3 days, the phase type, phase volume, and appearance of the aqueous phase in the test tube after reaching equilibrium are recorded. An emulsion liquid in between oil and water layers is taken out for observation under an optical microscope after being diluted with water at a 1:1 ratio.

(3) Zeta potential measurement and dynamic light scattering (DLS)

Zeta potential and nanoparticle aggregate size were measured by electrophoretic method and dynamic light scattering principle, respectively. The effect of different surfactants on the potential and particle size of the nano-solution was observed. Before the measurement, the tube was equilibrated at the desired temperature (25 °C) and the average was taken for three measurements.

(4) Contact Angle (CA) Measurement

The CA is a measure of the wetness of the core. During the measurement process, the clean core slices, with a thickness ranging from 1 to 2 mm, were immersed in the sample pool filled with kerosene. A syringe needle containing the test liquid was positioned directly above the core slices and submerged in the kerosene. By rotating the micro-injection device, small droplets of the test liquid (3~5 μ L) were gradually released, and images were captured at the moment when these droplets made initial contact with the core slices. Three measurements were performed, and their average value was taken.

(5) Interfacial tension (IFT) measurement

The IFT can be regarded as the contractile force acting on the liquid interface per unit length. The IFT between the imbibition fluids and simulated formation oil was measured at room temperature under a speed of 5500 r/min. Three measurements were conducted, and their average value was taken.

(6) Core imbibition experiment

The core imbibition experiment is used to test the final imbibition recovery degree of the different imbibition liquid systems. The core sample underwent washing, drying, weighing, vacuum treatment, saturation with formation water, and displacement method saturation with simulated oil. The weight change during each step was recorded to determine the saturated simulated oil quality. The saturated core was then placed into the imbibition bottle containing the imbibition liquid, and the change in oil volume was recorded over time. The imbibition recovery is calculated as the ratio of the volume of the displaced crude oil to the volume of the saturated crude oil, and expressed as a percentage.

3. Results and Discussion

3.1. Core Pore Structure and Major Mineral Composition

The T_2 spectrum of the core NMR and its corresponding porosity components are illustrated in Figure 1. The predominant pore type within the core samples is micro-nano pores, exhibiting a pore radius distribution ranging from 2 nm to 640 nm, which accounts for over 98% of the total pore volume and can be classified as ultra-small pores. Specifically, pores with a radius below 10 nm constitute approximately 19.23%, while those with a radius between 10 nm and 640 nm contribute to around 79.60%. This means that the core pore radius of the Chang 7 reservoir is small and the capillary force is large. In theory, it is suitable for spontaneous imbibition.

The main mineral composition and clay mineral analysis results of the core are shown in Figure 2 and Table 3. The main mineral is quartz (accounting for 47%), followed by plagioclase (accounting for 29.4%); the total amount of clay minerals is 8.5%, mainly chlorite and chlorite/Smectite mixed layer.

Table 3. XRD results of core mineral composition.

Quartz	Albite	Calcite	White Mica	Dolomite	Clay Minerals	Clay Mineral Content (%)				
(%)	(%)	(%)	(%)	(%)	(%)	K	C	I	I/S	C/S
47.0	29.4	11.6	3.3	0.2	8.5	13.3	32.1	17.1	9.4	28.1

K: Kaolinite; C: chlorite; I: Illite; I/S: Illite/Smectite mixed layer; C/S: chlorite/Smectite mixed layer.

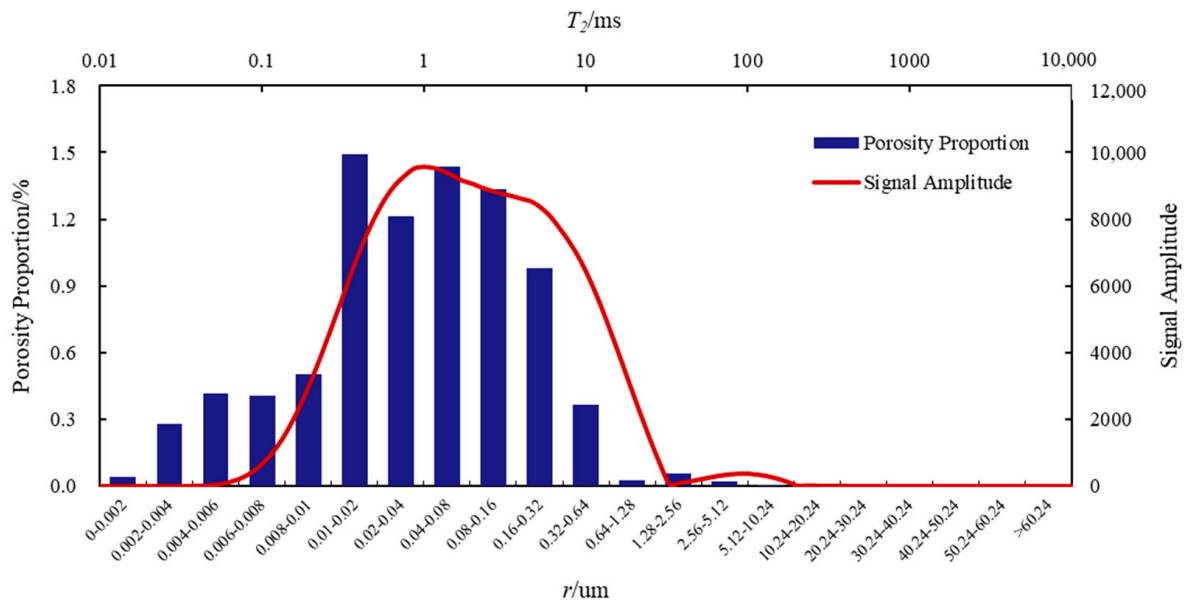


Figure 1. Core NMR T_2 spectrum and pore radius distribution.

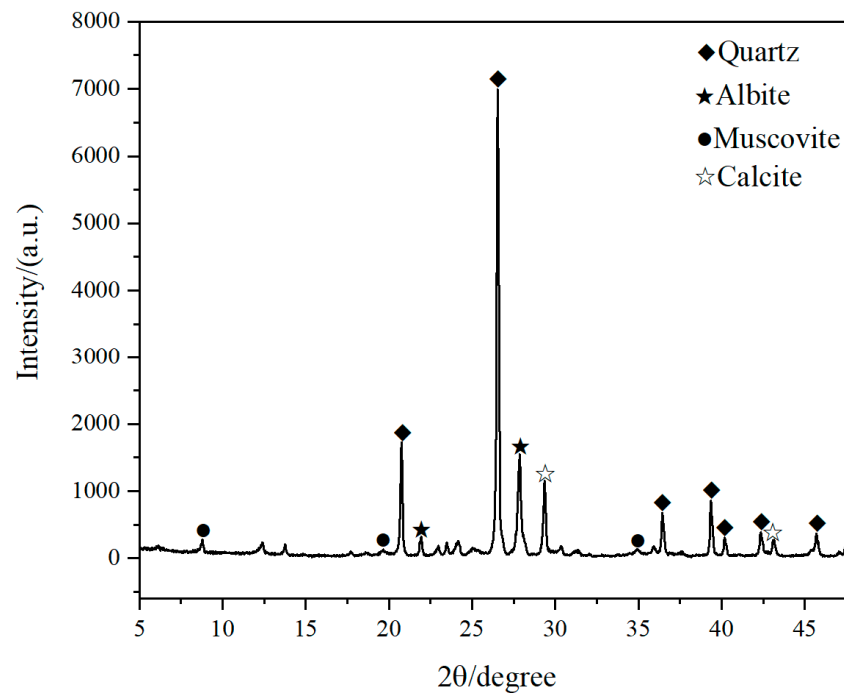


Figure 2. Core X-ray diffraction pattern.

In order to further analyze the pore structure of the core, SEM was employed to obtain the microscopic images of the core surface. As depicted in Figure 3, the mineral composition of the core is intricate and encompasses quartz, feldspar, calcite, and clay minerals, among others. The pore structure exhibits diversity with intergranular pores and intercrystalline pores being present. The overall intergranular pores of the core are well developed. Usually, such pores have good connectivity and can form an effective pore network. Figure 3A shows that the albite and honeycomb I/S mixed layer aggregates have pillow-like cemented interparticle pores; Figure 3B shows that the I/S mixed layer, quartz, and albite have cemented interparticle pores; Figure 3C shows that the plagioclase is dissolved into a residual form and the I/S mixed layer aggregates have cemented intergranular pores. Intergranular pores are often found in the interior of the particles. As shown in Figure 3D, the honeycomb I/S mixed layer aggregates

develop intercrystal pores, which are much smaller than interparticle pores and are usually blocked by organic matter or authigenic clay flakes, resulting in a lower effective porosity and poor connectivity [28].

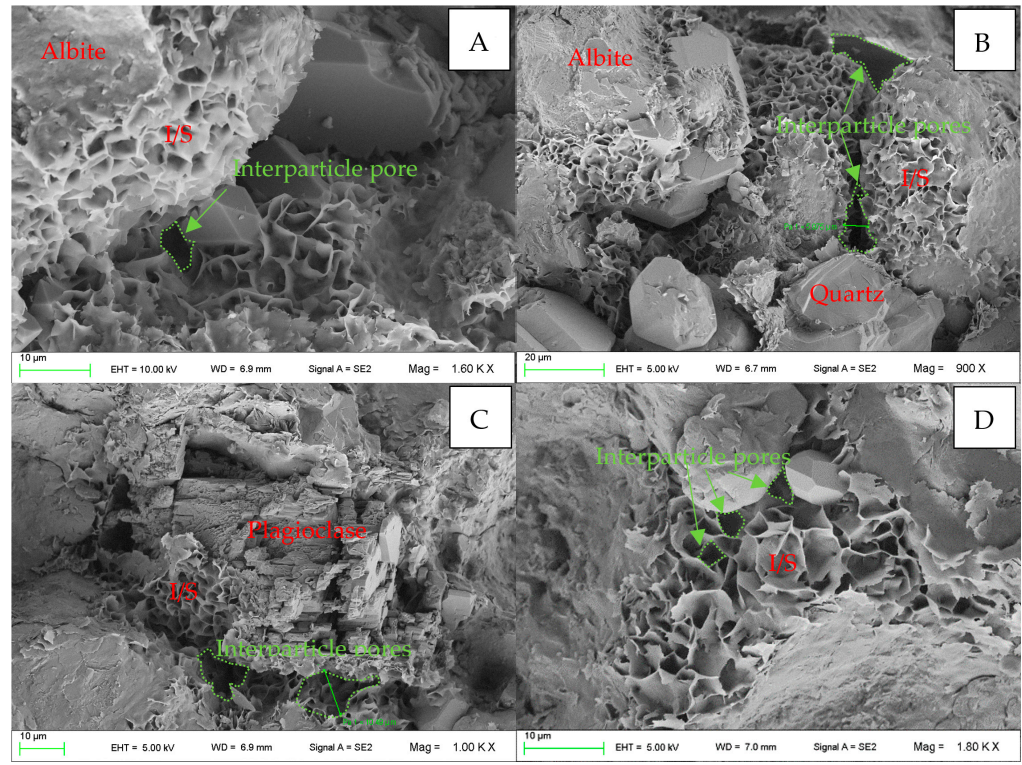


Figure 3. SEM image of characteristic pores in core reservoir (A–D).

3.2. Crude Oil Emulsification and Dispersion Experiment in an Imbibition System

The fully mixed oil–water system was left for three days and the changes in the oil–water phases are shown in Figure 4. The formation water and simulated oil were completely stratified and had a clear interface. The imbibition system with surfactants or nanomaterials had an intermediate emulsion layer, indicating that the imbibition solution and simulated oil had emulsified to different degrees. The emulsion stabilization effect after the addition of the nanomaterials was better than that without the nanoparticles, and the LAB + ZZ-1 emulsion layer was the thickest. The water phase of the LAB + ZZ-1 and AEO-7 + ZZ-1 systems became turbid, indicating that these two systems could disperse simulated oil into the water phase and have a better effect of the solubilizing emulsified crude oil.

The droplet morphology of the six imbibition fluid systems and the emulsified intermediate phase of the simulated oil diluted at 100× magnification is shown in Figure 5. The oil droplet diameter of the single surfactant system is about 10 μm. After the addition of the nanomaterials, the overall particle size of the oil droplets is smaller and more uniform. Among them, the AEO-7 + ZZ-1 system has the smallest oil droplet diameter with an average of about 1 μm, indicating that the system has the best effect in breaking and dispersing crude oil, followed by LAB + ZZ-1 with an average of about 5 μm. According to Figure 1, the pore throat radius of the experimental core is concentrated in 2 nm~5.12 μm, indicating that a large amount of the crude oil is contained in the tiny nanopore throat. After emulsification, the oil droplet diameter of the single surfactant system is large, the resistance through the pore throat is large, and the crude oil is difficult to recover. With the addition of the nanomaterials, the oil droplets are smaller in diameter and easier to pass through tiny pores and throats, resulting in a higher recovery rate. The AEO-7 + ZZ-1 system has good dispersing and emulsifying ability of crude oil, and the particle size of the emulsified crude oil is smaller, which is easier to be recovered through the pore throat.

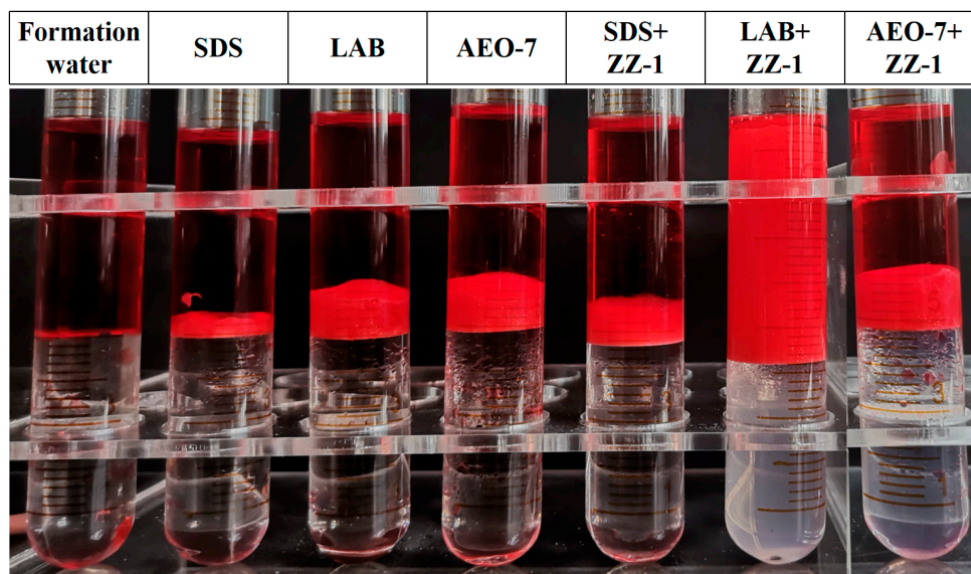


Figure 4. Testing of oil–water behavior in various imbibition fluid systems.

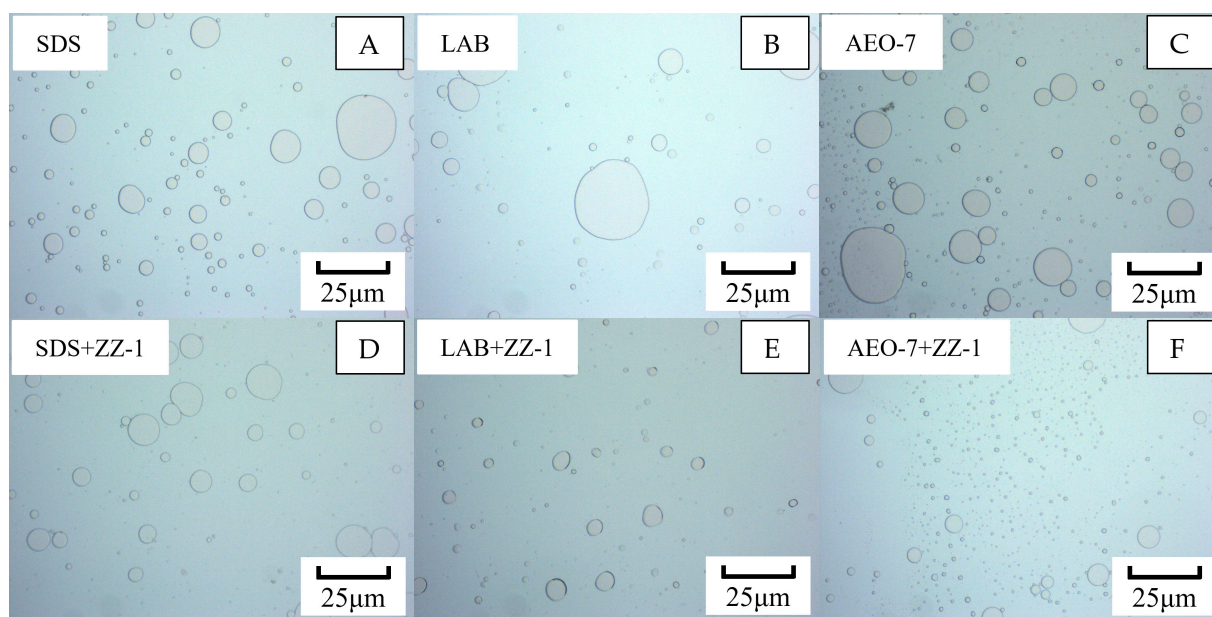


Figure 5. Microstructure of emulsion mixed with imbibition system and simulated oil under 100× magnification (A–F).

3.3. Zeta Potential Measurement and Dynamic Light Scattering (DLS)

Zeta potential is a measure of the strength of the mutual repulsion or attraction between particles, and is an important indicator to characterize the stability of dispersions. The smaller the molecule or dispersed particle is, the higher the absolute value of zeta potential (positive or negative) is, and the more stable the system is. Dynamic light scattering is one of the most common analytical methods used to determine the size and radius distribution of particles in suspensions or polymers in solution samples, and is commonly used to measure the size of nanoaggregates. Poly dispersity index (PDI) is a parameter that describes the uniformity of particle size distribution. The smaller the value of PDI, the more uniform the particle size distribution. Conversely, the larger the value of PDI is, the more uneven the particle size distribution is.

In general, the adsorption of surfactants on the surface of nanoparticles affects the electrostatic and steric interactions between nanoparticles and surfactant molecules. The

zeta potential, size, and poly dispersity index (PDI) of the nanoaggregates of the individual nanoparticles and the different surfactants and nanoparticle composite systems were measured, and the results are shown in Table 4.

Table 4. Zeta potential of different systems and sizes of nanoaggregates.

	Zeta Potential (mV)		Sizes (Z-Average) (nm)		PDI	
	After Preparation	After 7 Days	After Preparation	After 7 Days	After Preparation	After 7 Days
ZZ-1	−32.3	−22.6	15.3	29.8	0.198	0.285
SDS + ZZ-1	−59.5	−55.1	58.3	125.6	0.483	0.650
LAB + ZZ-1	−28.5	−15.3	103.8	362.9	0.202	0.267
AEO-7 + ZZ-1	−31.5	−29.8	25.7	33.06	0.187	0.237

As can be seen from the zeta potential, the surface of the nanoparticles is negatively charged (−32.3 mV), and after the addition of the surfactant, the zeta potential value of the solution changes, but the potential is still negative (SDS + ZZ-1 −59.5 mV, LAB + ZZ-1 −28.5 mV, and AEO-7 + ZZ-1 −31.5 mV). After 7 days, the absolute value of the zeta potential of the solution decreased, indicating that the solution was unstable and there was a formation of nanoaggregates, but the absolute value was greater than 15 mV. From the perspective of electrostatic, the nano-dispersion was in a relatively stable state [29].

The addition of anions increases the absolute value of zeta potential, which indicates that the electrostatic repulsion is high and the solution is stable under the action of anionic surfactants. The adsorption of the anionic surfactants on the surface of the nanoparticles resulted in the increase in the total negative charge and zeta potential of the aggregate surface. At the same time, it is observed that the particle size increases after the anionic surfactant is added, which may be due to the electrostatic repulsion leading to the desorption of the nanoparticles from the interface of the nanoparticles and surfactants and adsorption to the aggregates, which increases the size of the nanoaggregate in the bulk solution [30].

The addition of the zwitterionic surfactant LAB reduced the absolute zeta potential of the system and increased the particle size of the nanoaggregate. This is because the positive charge formed by LAB in the solution and the negative charge on the surface of the nanoparticles are prone to electrostatic attraction, and the adsorption of the surfactant molecules on the surface of the nanoparticles increases, so the stability of the system is poor, and the particle size of the nanoparticles increases.

Compared with other types of surfactants, the aggregate size of the non-ionic surfactants with the nanoparticles was significantly reduced, and fewer nanoaggregates were formed in the solution. This result is consistent with the above experimental results of oil dispersibility. However, the lower zeta potential value of the mixture of the nanoparticles and AEO-7 is due to the insignificant interaction between the non-ionic surfactant and the charged surface of the nanoparticles [30]. The stability of nanoparticle–non-ionic surfactant mixtures is mainly achieved by steric stabilization rather than electrostatic interactions [29]. The DLS measurement results show that the non-ionic surfactant has better dispersion stability.

The PDI of the four systems after 7 days of configuration was greater than that at the beginning of the configuration, indicating that the size of the nanoparticles changed after agglomeration, and the particle size distribution became uneven. However, the PDI value of all the nanoparticle dispersions was less than 0.7, indicating that the particle size uniformity of the system was relatively good.

3.4. CA and IFT of Imbibition Fluid System

(1) Contact Angle

Wettability is an important factor in imbibition. If the core is more hydrophilic, the imbibition solution system is more likely to enter the micropores and replace the crude oil

under capillary force. The initial wettability of the six cores is highly hydrophilic. After the imbibition experiment, the wettability angle between the imbibition solution and the core is measured again and the results are shown in Figure 6.

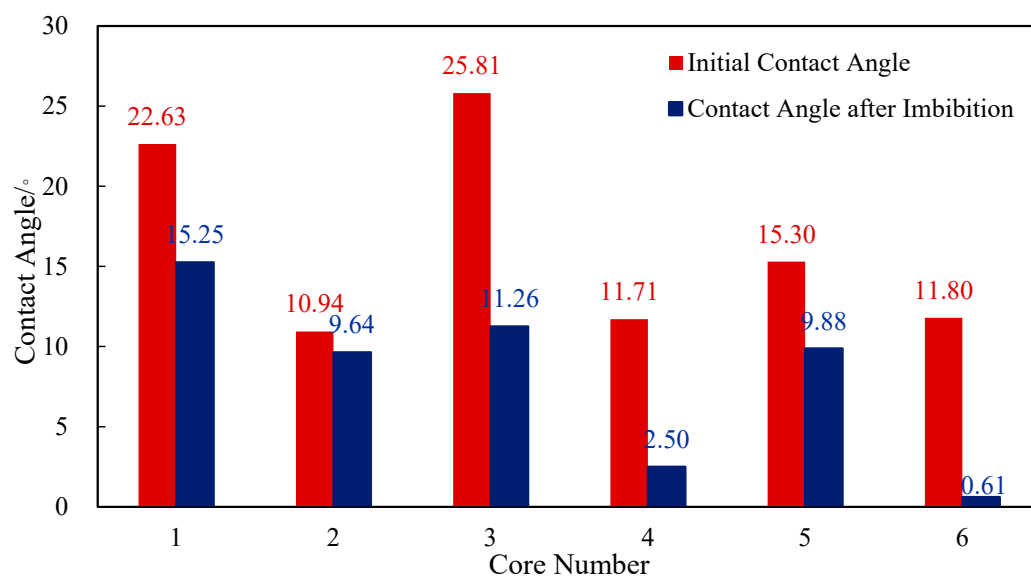


Figure 6. Changes in contact angle before and after imbibition.

It can be seen that after imbibition, the wettability of the core is improved to varying degrees under the action of the imbibition fluid and the CA becomes smaller, indicating that the hydrophilicity of the core increases. The greatest change in wettability is found in cores No. 3 and No. 6, which correspond to the surfactant system of AEO-7 (non-ionic), CA decreased from 25.81 to 11.26 and from 11.80 to 0.61; followed by SDS (anionic), CA decreased from 22.63 to 15.25 and from 11.71 to 2.50; and LAB (amphoteric ionic) has the worst effect in improving wettability with CA decreased from 10.94 to 9.64 and from 15.30 to 9.88. For anionic surfactants, the change in wettability is mainly based on the theory of “ion pair formation” [31]. The negatively charged hydrophilic groups in the surfactants can form “ion pairs” with the oil film and polar substances adsorbed on the rock surface through the action of the electric field force, and strip these oil-wet substances from the rock surface to achieve the purpose of improving wettability [32,33]. For surfactants with emulsifying ability, by reducing the IFT between oil and water, the oil film tends to roll slowly and finally detach from the surface to form an emulsion, showing a strong ability to dissolve and start oil droplets, and achieve the effect of improving wettability in another way [34].

After the addition of nanomaterials, due to the adsorption and structural separation pressure of nanoparticles, the imbibition fluid system has a certain degree of improvement in improving wettability compared to the single surfactant system. The theory of “structural separation pressure” was proposed by Darsh Wasan [35,36]. The principle is that nanoparticles form an ordered structural layer in the wedge region of a three-phase contact due to Brownian motion and electrostatic repulsion. This wedge structure can produce forward thrust, namely structural separation pressure, which increases with decreasing film thickness and thus drives the nanofluids to flow towards the wedge tip, reinforcing the dynamic expansion of the nanoparticles on the rock surface and promoting the peeling of the oil droplets from the rock.

(2) Interfacial tension

The IFT of the surfactant system before and after the addition of the nanomaterials is shown in Figure 7. After the addition of the nanomaterials, the IFT of the solution is reduced and the largest reduction is for AEO-7 with the IFT value reduced from $0.9190 \text{ mN}\cdot\text{m}^{-1}$ to $0.1750 \text{ mN}\cdot\text{m}^{-1}$, a reduction of 81%; followed by SDS with a reduction of

15.9%; and the smallest reduction is for LAB with a reduction of 6.2%. The lower interfacial tension means that the oil droplets have a better deformation ability and can pass through the tiny pore throat more easily. This is consistent with the research of Yekeen et al. [30], Kumar [37], and Kuang [38], which showed that there is competitive adsorption between nanomaterials and surfactants at the interface. In the process of competitive adsorption, the nanoparticle–non-ionic surfactant mixture can be better adsorbed and aggregated at the oil–water interface of the nanoparticle–surfactant aqueous solution, thereby reducing the oil–water IFT. Therefore, compared to other fluids, the nanoparticle–non-ionic surfactant fluid is an ideal colloidal solution for reducing the oil–water IFT.

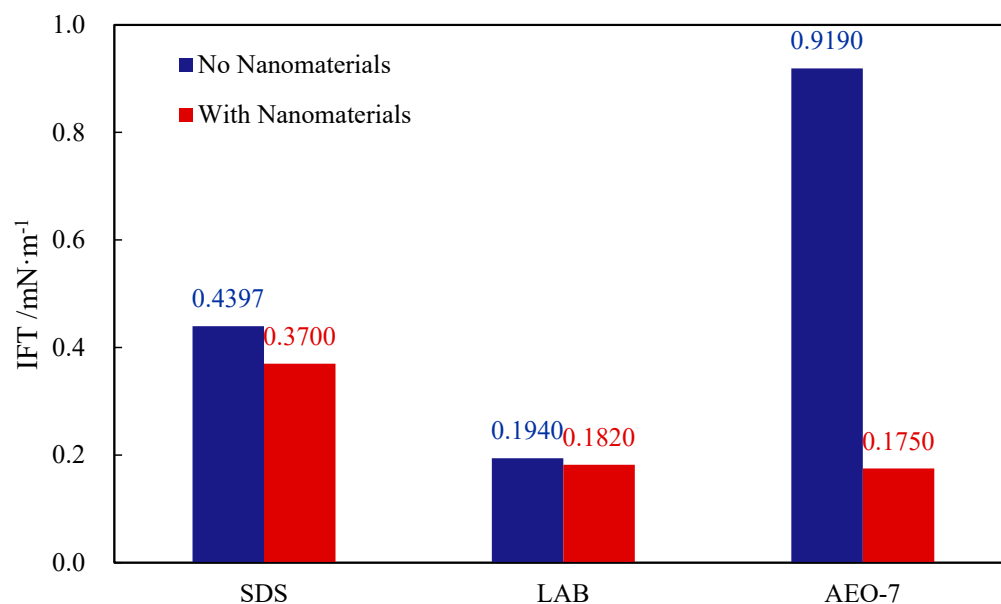


Figure 7. IFT of surfactant system before and after adding nanomaterials.

3.5. Spontaneous Core Imbibition Experiment

(1) Imbibition Recovery

Six cores were placed in the prepared imbibition solution system of the single surfactant and the imbibition solution system of the surfactant + nanomaterials, respectively, and the changes in oil volume over time were recorded. The results are shown in Figure 8.

It can be seen that with the increase in time, the volume of the produced oil and imbibition recovery are increasing. Furthermore, the recovery of the imbibition systems with the nanoparticles is higher than that of the non-nanoparticles, which indicates that the nanoparticles have a positive effect on improving oil recovery with the synergistic effect of the surfactants. But the imbibition speed is lower, and the imbibition equilibrium time is also prolonged accordingly when the nanoparticles are added. Before the addition of the nanomaterials, the imbibition recovery from high to low is LAB (31.54%) > SDS (30.21%) > AEO-7 (25.29%); after the addition of the nanomaterials, the imbibition recovery from high to low is as follows: AEO-7 + ZZ-1 (49.27%) > SDS + ZZ-1 (43.07%) > LAB + ZZ-1 (39.68%). Therefore, the nanomaterials have the best synergistic effect with the anionic surfactant on improving the imbibition recovery, and next are the anionic and zwitterionic surfactants.

According to the above experimental results, it may be that the nanoparticles and anionic surfactant system have smaller particle size, lower CA and IFT, and are easier to enter into the tiny pore throat to replace the crude oil.

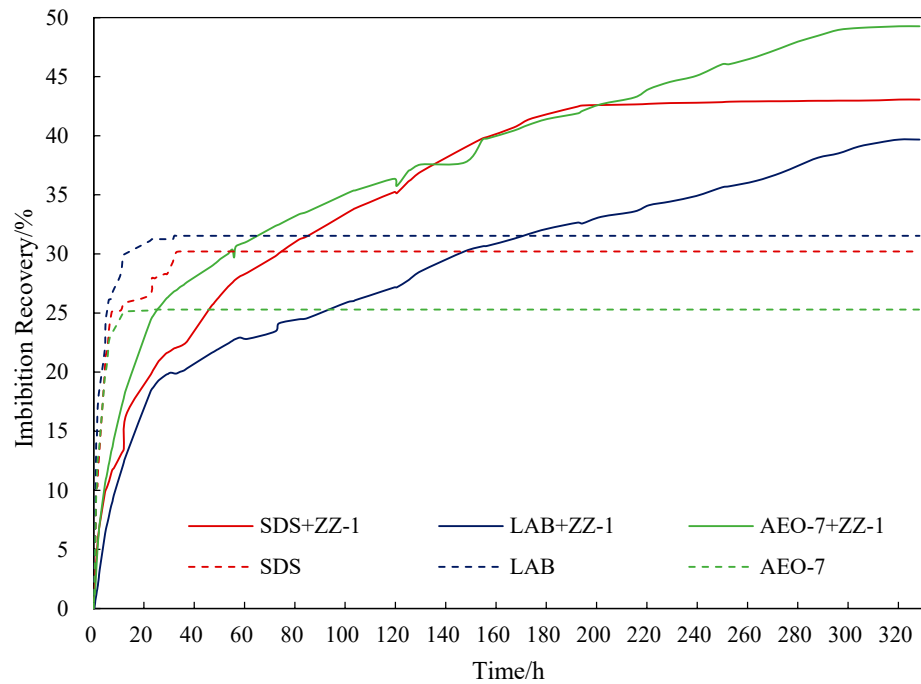


Figure 8. Curves of variation in imbibition recovery over time.

(2) Increasing times of imbibition recovery

To quantify the extent of the influence of the nanomaterials on the sorption recovery of the surfactant system, the following definition is made:

Increasing times of imbibition = (Recovery of fluids with nanomaterials – Recovery of fluids without nanomaterials)/Recovery of fluids with nanomaterials

The larger the increasing times of the imbibition recovery, the better the effect of the nanomaterials on enhancing the imbibition of the surfactant. The imbibition recovery and the increasing times of the imbibition recovery of each system are shown in Figure 9. After adding nano-silica sol, the imbibition recovery of the non-ionic surfactant system AEO-7 increased the most, with an increase of 0.948; followed by the anionic surfactant system SDS, with an increase of 0.425; and the lowest was the amphoteric ionic surfactant system LAB, with an increase of 0.258. It also shows that the effect of the nanoparticle and anionic surfactant system is the best, and the ability to improve the oil recovery is the strongest.

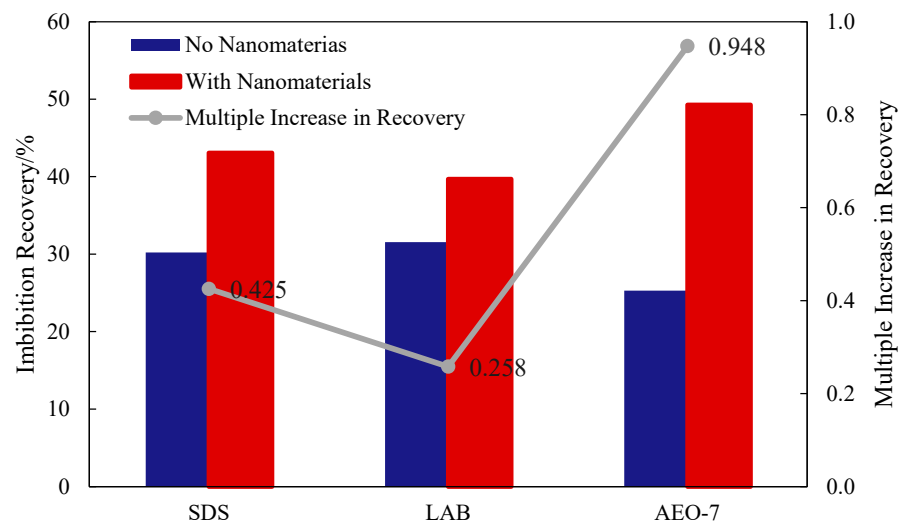


Figure 9. Imbibition recovery and increasing times of imbibition recovery.

(3) Adhesion work

Adhesion work refers to the work required to remove crude oil adsorbed on the core pore surface. In the process of imbibition oil displacement, under the same oil displacement power, the smaller the required adhesion work is, the better the oil displacement effect is. The adhesion work is related to the interface tension and CA as follows:

$$W_a = \sigma_{ow}(1 - \cos\theta) \quad (1)$$

W_a —the adhesive work required for the detachment of crude oil from a rock surface, J;
 θ —contact angle, °;

σ_{ow} —oil–water interfacial tension, $\text{mN}\cdot\text{m}^{-1}$.

As can be seen from Equation (1), the smaller the oil–water IFT and CA, the smaller the required adhesive work, the easier the oil droplets are to be stripped off from the rock surface, and the higher the oil washing efficiency is. The adhesive work and the final imbibition recovery of the six imbibition systems are shown in Figure 10.

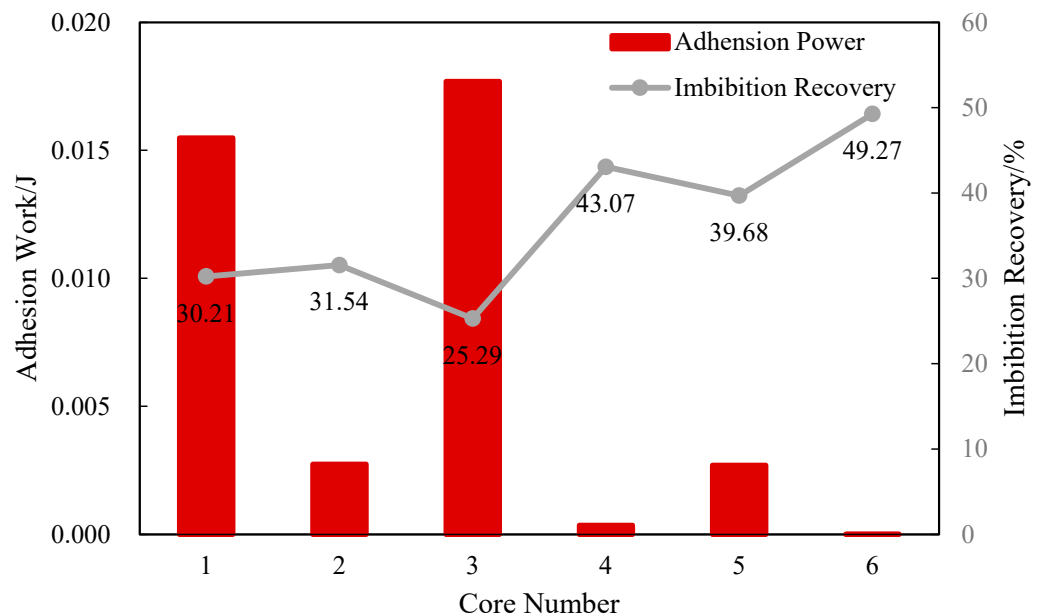


Figure 10. Adhesion work and imbibition recovery of different systems.

It can be seen that the adhesion work of the imbibition solution system with the nanomaterials is lower than that of the single surfactant system. The adhesion work of the SDS, LAB, and AEO-7 were 1.5×10^{-2} J, 2.7×10^{-3} J, and 1.8×10^{-2} J, respectively, before the nanomaterials were added. After adding the nanomaterials, the adhesion work is 3.5×10^{-4} J, 2.7×10^{-3} J, and 9.9×10^{-6} J, respectively. The adhesive work is negatively correlated with the final imbibition recovery. The lower the adhesive work is, the higher the final imbibition recovery is. The system of the surfactant with the nanoparticles has the lowest adhesion work and the highest recovery.

4. Conclusions

The composite system of nanomaterial and surfactant shows excellent performance in spontaneous imbibition recovery. The specific conclusions are as follows:

- (1) Nanomaterials can promote the dispersion and emulsification of crude oil in surfactant system. After the addition of nanomaterials, the dispersion effect of crude oil is better and the particle size of crude oil is smaller. The nano-silica sol has the best dispersion effect on non-ionic surfactant AEO-7.
- (2) The results of zeta potential and DLS test show that different surfactants have great influence on the stability and particle size of nano-silica sol. The anionic surfactants

increase the repulsive force and makes the system more stable with the zeta potential increasing from -32.3 mV to -59.5 mV, but the size of the nanoaggregates increases from 15.3 nm to 58.3 nm due to the nanoparticles' adsorption to the aggregates which is desorption from the interface. The positive charge of zwitterionic surfactant attracts the negative charge of nanoparticle surface, which causes particle size to increase from 15.3 nm to 103.8 nm. Non-ionic surfactants exhibit better stability and smaller particle size because of the insignificant interaction between the non-ionic surfactant and the charged surfaces of the particles.

- (3) Nanomaterials can enhance the ability of surfactant system to improve wettability and reduce IFT, and the non-ionic surfactant AEO-7 has the best property with the synergism of nanoparticles which has the smallest CA with 0.61° and the lowest IFT with 0.1750 mN·m⁻¹.
- (4) Nanomaterials can improve the spontaneous imbibition recovery of surfactant system. The increase of imbibition recovery from high to low is AEO-7 (0.948 times) > SDS (0.425 times) > LAB (0.258 times). It is found that the imbibition recovery rate is closely related to the emulsification, dispersibility, particle size, contact angle, and interfacial tension of imbibition liquid system.
- (5) The addition of nanomaterials can reduce the adhesion work of the system, which is negatively correlated with the final imbibition recovery.
- (6) The composite system of nanoparticles and surfactants has great application potential in tight oil development. However, during the imbibition process, a large number of nanoparticles remain underground and cannot be discharged, so reservoir damage is a serious problem. In the future, more research should be focused on the compatibility of nano-systems and reservoirs, so as to reduce reservoir damage and develop lower-cost nano-systems.

Author Contributions: Formal analysis, X.W. (Xinmeng Wu); Data curation, Y.Z., X.F. and J.X.; Writing—original draft, X.W. (Xiaoxiang Wang); Writing—review & editing, X.W. (Xiaoxiang Wang); Supervision, D.Z. All authors have read and agreed to the published version of the manuscript.

Funding: This research was funded by the National Natural Science Foundation of China, grant number U23B2089, 51934005.

Data Availability Statement: We state that the data is unavailable due to privacy or ethical restrictions of the company and university.

Conflicts of Interest: Authors Yang Zhang and Xin Fan were employed by the company Oil Production Plant 11 of Petro China Changqing Oilfield Company and Xinmeng Wu was employed by the company South Sulige Operating Company of CNPC Changqing Oilfield. The remaining authors declare that the research was conducted in the absence of any commercial or financial relationships that could be construed as a potential conflict of interest. The Oil Production Plant 11 of Petro China Changqing Oilfield Company and South Sulige Operating Company of CNPC Changqing Oilfield had no role in the design of the study; in the collection, analyses, or interpretation of data; in the writing of the manuscript, or in the decision to publish the results.

References

1. Tianru, W. Research on Influence Law of Imbibition Process and Mechanism of Matrix Crude Oil Migration by Slick-Water Fracturing Fluid in Tight Reservoirs. Master's Thesis, China University of Geosciences Beijing, Beijing, China, 2020.
2. Xuewu, W.; Pufu, X.; Bin, Y.; Zhizeng, X.; Fei, L.; Shuming, Y. Recovery Law and Micro Mechanism of High Pressure Imbibition in Tight Core. *J. Shengli Coll. China Univ. Pet.* **2021**, *35*, 46–49.
3. Xuepeng, Z. Preparation and Application of Surfactant Used in Imbibition for Fracturing. Master's Thesis, Shaanxi University of Science and Technology, Xi'an, China, 2019.
4. Yixing, W. Study on the Spontaneous Imbibition Effect of Tight Sandstone Gas Reservoirs in Sulige. Master's Thesis, Xi'an Shiyou University, Xi'an, China, 2019.
5. Ke, L.; Hongfu, F.; Biao, Y.; Guodong, W. Progress in Mechanism and Technology of Imbibition Recovery in Low Permeability Reservoirs. *Oilfield Chem.* **2023**, *40*, 182–190.
6. Shiming, W.; Yan, J.; Yang, X.; Dan, X.; Ping, Z. Influence of spontaneous imbibition on post-fracturing well soaking in shale oil reservoirs. *Oil Drill. Prod. Technol.* **2023**, *45*, 756–765.

7. Yingxian, L.; Zhihua, Y.; Baocai, Z. Study on surfactant combination system suitable for chemical flooding in low permeability reservoirs. *Energy Chem. Ind.* **2018**, *39*, 40–43.
8. Zhiyu, W.; Zhanwu, G.; Shuwei, M.; Jiyong, Z.; Jianchao, S.; Zhen, L. Preliminary study on imbibition and oil displacement of Chang 7 shale oil in Ordos Basin. *Nat. Gas Geosci.* **2021**, *32*, 1874–1879.
9. Tongxiu, S. Research on the Dynamic Wetting in Functional Surfactant Flooding. Master's Thesis, China University of Petroleum (East China), Qingdao, China, 2018.
10. Chuanliang, L.; Wanyi, M.; Tingxin, W.; Suyang, Z. A Study on Mechanism of Oil Displacement by Imbibition. *Xinjiang Pet. Geol.* **2019**, *40*, 687–694.
11. Fuyong, W.; Kun, Y. Influence of pore throat size distribution on oil displacement by spontaneous imbibition in tight oil reservoirs. *Lithol. Reserv.* **2021**, *33*, 155–162.
12. Liantong, S. Imbibition and Oil Displacement Mechanism of Micro-nano Pores in Tight Reservoir. Master's Thesis, China University of Geosciences Beijing, Beijing, China, 2021.
13. Ming, L. Study on the Spontaneous Imbibition Effect of Fracturing Fluid in Chang 7 Reservoir. Master's Thesis, Xi'an Shiyou University, Xi'an, China, 2018.
14. Lihua, S.; Dengfeng, W.; Yuwen, C.; Hailong, D.; Tao, D.; Tiaotiao, S.; Feifei, W. Micro imbibition mechanism experiment of tight reservoir based on microfluidic model. *J. China Univ. Pet. (Ed. Nat. Sci.)* **2023**, 1–12.
15. Biao, W.; Taiwei, L.; Jianye, Y.; Zhipeng, D.; Jie, Z. Analysis of imbibition mechanism and influencing factors of surfactant displacement in shale oil reservoirs. *Pet. Geol. Recovery Effic.* **2023**, *30*, 92–103.
16. Lihua, S.; Ying, X.; Pengxing, C.; Tongyu, W.; Binchi, H. Spontaneous static imbibition experiment of tight reservoir and its influencing factors. *Sci. Technol. Eng.* **2023**, *23*, 12494–12503.
17. Xiangqian, H.; Yongjun, L.; Bo, F.; Fuxiang, Z.; Guangjun, H.; Tao, Z.; Hongsheng, M. Research status and prospect of modified nano-SiO₂ for imbibition flooding. *Mod. Chem. Ind.* **2023**, *43*, 84–88+93.
18. Suleimanov, B.A.; Ismailov, F.S.; Veliyev, E.F. Nanofluid for enhanced oil recovery. *J. Pet. Sci. Eng.* **2011**, *78*, 431–437. [[CrossRef](#)]
19. Jiang, K.; Xiong, C.; Ding, B.; Geng, X.; Liu, W.; Chen, W.; Huang, T.; Xu, H.; Xu, Q.; Liang, B. Nanomaterials in EOR: A Review and Future Perspectives in Unconventional Reservoirs. *Energy Fuels* **2023**, *37*, 10045–10060. [[CrossRef](#)]
20. Al-Asadi, A.; Rodil, E.; Soto, A. Nanoparticles in Chemical EOR: A Review on Flooding Tests. *Nanomaterials* **2022**, *12*, 4142. [[CrossRef](#)] [[PubMed](#)]
21. Hou, X.Y.; Sheng, J.J. Properties, preparation, stability of nanoemulsions, their improving oil recovery mechanisms, and challenges for oil field applications-A critical review. *Geoenergy Sci. Eng.* **2023**, *221*, 211360. [[CrossRef](#)]
22. Hongru, L.; Xiangguo, L.; Xiaoyan, W.; Qingguo, Y.; Yu, L.; Bao, C. Effect and Mechanism of Nano Oil Displacement Agent on Enhancing Oil Recovery. *Oilfield Chem.* **2023**, *40*, 305–311.
23. Tuo, L.; Huipeng, W.; Chen, H.; Changhua, Y.; Ming, Q.; Jirui, H.; Erlong, Y.; Mingxing, B. Mechanism of oil film stripping by active MoS₂ nanosheets. *Pet. Geol. Recovery Effic.* **2024**, *32*, 138–147.
24. Jiashun, G.; Jinfeng, L.; Qian, L.; Qian, W.; Tingqiang, C.; Feifei, H.; Jia, W. Preparation of Novel Nanocomposite Polymer PADD-1 and Its Application in Fracturing Fluid. *Drill. Prod. Technol.* **2023**, *46*, 133–139.
25. Shuai, Y.; Fujian, Z.; Yuan, L.; Xingyuan, L.; Tianbo, L.; Erdong, Y. Mechanism of imbibition and production enhancement of nanoemulsion in tight sandstone oil reservoirs. *Pet. Geol. Recovery Effic.* **2024**, *31*, 126–136.
26. Wenjiao, L. Study on Regulation of Silica Nanoparticles Surface Chemical Property by Using Surfactant and Imbibition Mechanism. Master's Thesis, China University of Petroleum (East China), Qingdao, China, 2019.
27. Chaudhury, M.K. Spread the word about nanofluids. *Nature* **2003**, *423*, 131–132. [[CrossRef](#)] [[PubMed](#)]
28. Wang, Y.; Zhu, Y.; Chen, S.; Li, W. Characteristics of the Nanoscale Pore Structure in Northwestern Hunan Shale Gas Reservoirs Using Field Emission Scanning Electron Microscopy, High-Pressure Mercury Intrusion, and Gas Adsorption. *Energy Fuels* **2014**, *28*, 945–955. [[CrossRef](#)]
29. White, B.; Banerjee, S.; O'Brien, S.; Turro, N.J.; Herman, I.P. Zeta-Potential Measurements of Surfactant-Wrapped Individual Single-Walled Carbon Nanotubes. *J. Phys. Chem.* **2007**, *37*, 13684–13690. [[CrossRef](#)]
30. Yekeen, N.; Padmanabhan, E.; Idris, A.K. Synergistic effects of nanoparticles and surfactants on n-decane-water interfacial tension and bulk foam stability at high temperature. *J. Pet. Sci. Eng.* **2019**, *179*, 814–830. [[CrossRef](#)]
31. Junrong, L. Imbibition in Shale Oil Reservoirs Mechanisms of Surfactant-Enhanced Imbibition in Shale Oil Reservoirs Mechanisms of Surfactant-Enhanced. Ph.D. Thesis, China University of Petroleum, Beijing, China, 2021.
32. Liu, J.; Sheng, J.J.; Wang, X.; Ge, H.; Yao, E. Experimental study of wettability alteration and spontaneous imbibition in Chinese shale oil reservoirs using anionic and nonionic surfactants. *J. Pet. Sci. Eng.* **2019**, *175*, 624–633. [[CrossRef](#)]
33. Salehi, M.; Johnson, S.J.; Liang, J.-T. Mechanistic Study of Wettability Alteration Using Surfactants with Applications in Naturally Fractured Reservoirs. *Langmuir* **2008**, *24*, 14099–14107. [[CrossRef](#)] [[PubMed](#)]
34. Kao, R.L.; Wasan, D.T.; Nikolov, A.; Edwards, D.A. Mechanisms of Oil Removal from a Solid Surface in the Presence of Anionic Micellar Solutions. *Colloids Surf.* **1988**, *34*, 389–398. [[CrossRef](#)]
35. Wasan, D.T.; Nikolov, A.D. Spreading of nanofluids on solids. *Nature* **2003**, *423*, 156–159. [[CrossRef](#)] [[PubMed](#)]
36. Wasan, D.T.; Nikolov, A.; Kondiparty, K. The wetting and spreading of nanofluids on solids: Role of the structural disjoining pressure. *Curr. Opin. Colloid Interface Sci.* **2011**, *16*, 344–349. [[CrossRef](#)]

37. Kumar, S.J.; Mandal, A. Studies on interfacial behavior and wettability change phenomena by ionic and nonionic surfactants in presence of alkalis and salt for enhanced oil recovery. *Appl. Surf. Sci.* **2016**, *372*, 42–51. [[CrossRef](#)]
38. Kuang, W.; Saraji, S.; Piri, M. A systematic experimental investigation on the synergistic effects of aqueous nanofluids on interfacial properties and their implications for enhanced oil recovery. *Fuel* **2018**, *220*, 849–870. [[CrossRef](#)]

Disclaimer/Publisher’s Note: The statements, opinions and data contained in all publications are solely those of the individual author(s) and contributor(s) and not of MDPI and/or the editor(s). MDPI and/or the editor(s) disclaim responsibility for any injury to people or property resulting from any ideas, methods, instructions or products referred to in the content.